



## UvA-DARE (Digital Academic Repository)

### Physiological and genetic studies towards biofuel production in cyanobacteria

Schuurmans, R.M.

**Publication date**

2017

**Document Version**

Other version

**License**

Other

[Link to publication](#)

**Citation for published version (APA):**

Schuurmans, R. M. (2017). *Physiological and genetic studies towards biofuel production in cyanobacteria*. [Thesis, fully internal, Universiteit van Amsterdam].

**General rights**

It is not permitted to download or to forward/distribute the text or part of it without the consent of the author(s) and/or copyright holder(s), other than for strictly personal, individual use, unless the work is under an open content license (like Creative Commons).

**Disclaimer/Complaints regulations**

If you believe that digital publication of certain material infringes any of your rights or (privacy) interests, please let the Library know, stating your reasons. In case of a legitimate complaint, the Library will make the material inaccessible and/or remove it from the website. Please Ask the Library: <https://uba.uva.nl/en/contact>, or a letter to: Library of the University of Amsterdam, Secretariat, P.O. Box 19185, 1000 GD Amsterdam, The Netherlands. You will be contacted as soon as possible.

# Chapter 2

---

## **The redox potential of the plastoquinone pool of the cyanobacterium *Synechocystis* sp. PCC 6803 is under strict homeostatic control**

*R. Milou Schuurmans<sup>1</sup>, J. Merijn Schuurmans<sup>2</sup>, Martijn Bekker<sup>1</sup>, Jacco C. Kromkamp<sup>3</sup>, Hans C.P. Matthijs<sup>2</sup>, Klaas J. Hellingwerf<sup>1</sup>*

<sup>1</sup>*Swammerdam Institute for Life Sciences, University of Amsterdam, Science Park 904, 1098 XH, Amsterdam, The Netherlands*

<sup>2</sup>*Institute for Biodiversity and Ecosystem Dynamics, University of Amsterdam, Science Park 904, 1098 XH, Amsterdam, The Netherlands.*

<sup>3</sup>*Royal Netherlands Institute for Sea Research, Koringaweg 7, 4401 NT, Yerseke, The Netherlands*

This chapter was published as:

Schuurmans RM, Schuurmans JM, Bekker M, Kromkamp JC, Matthijs HCP, Hellingwerf KJ. The Redox Potential of the Plastoquinone Pool of the Cyanobacterium *Synechocystis* Species Strain PCC 6803 Is under Strict Homeostatic Control. *Plant Physiol.* 2014;165: 463-475.

## Abstract

A method is presented for rapid extraction of the total plastoquinone pool from *Synechocystis* sp. PCC 6803 cells that preserves the *in vivo* plastoquinol (PQH<sub>2</sub>) to plastoquinone (PQ) ratio. Cells were rapidly transferred into ice-cold organic solvent for instantaneous extraction of the cellular PQ plus PQH<sub>2</sub> content. After HPLC fractionation of the organic-phase extract, the plastoquinol content was quantitatively determined via its fluorescence emission at 330 nm. The *in cell* PQH<sub>2</sub>/PQ ratio then followed from comparison of the PQH<sub>2</sub> signal in samples as collected, and in an identical sample after complete reduction with sodium borohydride.

Prior to PQ(H<sub>2</sub>) extraction, cells from steady state chemostat cultures were exposed to a wide range of physiological conditions, including high/low availability of inorganic carbon, and various actinic illumination conditions. Well-characterized electron-transfer inhibitors were used to generate a reduced or an oxidized PQ pool for reference.

The *in vivo* redox state of the PQ pool was correlated with the results of PAM-based chlorophyll *a* fluorescence emission measurements, oxygen exchange rates, and 77K fluorescence emission spectra. Our results show that the redox state of the PQ pool of *Synechocystis* sp. PCC 6803 is subject to strict homeostatic control, *i.e.* regulated between narrow limits, in contrast to the more dynamic chlorophyll *a* fluorescence signal.

## Key words

Plastoquinol extraction, PQ-pool, photosynthesis, photo-bioreactor, LED lighting, 77K fluorescence spectra, membrane inlet mass spectrometry (MIMS).

## Abbreviations

PQ, plastoquinone; PQH<sub>2</sub>, plastoquinol; PQ pool, sum of PQ and PQH<sub>2</sub>; PBS, phycobilisomes; LHC, light harvesting complex; DCMU, 3-(3,4-dichlorophenyl)-1,1-dimethylurea, DCBQ, 2,6-dichlorobenzoquinone; DBMIB, 2,5-dibromo-3methyl-6-isopropyl-p-benzoquinone; MIMS, membrane inlet mass spectroscopy.

## Introduction

The photosynthetic apparatus of oxygenic phototrophs consists of two types of photosynthetic reaction centres: photosystem II (PSII) and photosystem I (PSI). Both photosystems are connected in series, with electrons flowing from PSII towards PSI through an intermediate electron transfer chain, which comprises the so-called plastoquinone pool (PQ pool), plastocyanin and/or cytochrome  $c_{553}$ , and the cytochrome  $b_6f$  complex. The redox potential of the PQ pool is clamped by the relative rates of electron release into and uptake from this pool. Within the PSII complex electrons are extracted from water at the luminal side of the thylakoid membrane and transferred to the primary accepting quinone,  $Q_A$ , at the stromal side. The electron is subsequently transferred to a plastoquinone molecule in the  $Q_B$  site of PSII. The intermediate  $Q_B$  semiquinone, which is formed accordingly is stable in the  $Q_B$  site for several seconds [81,82] and can subsequently be reduced to plastoquinol (PQH<sub>2</sub>). The midpoint potential of  $Q_A$  reduction is approximately -100 mV [83,84], whereas the corresponding midpoint potential of the  $Q_B$  semiquinone is close to zero [85]. Plastoquinol equilibrates with the PQ pool in the thylakoid membranes, which has a size that is approximately one order of magnitude larger than the number of PSII reaction centres [86,87].

PQ is a lipophilic, membrane-bound electron carrier, with a midpoint potential of +80 mV [88] that can accept 2 electrons and 2 protons, to form PQH<sub>2</sub> [89]. PQH<sub>2</sub> can donate both electrons to the cytochrome  $b_6f$  complex; one to cytochrome  $b_6$  LP (low potential), by which reduced cytochrome  $b_6$  HP (high potential) is formed, and one to the cytochrome  $f$  moiety on the luminal side of the thylakoid membrane, where the 2 protons are released. Cytochrome  $b_6$  HP then donates an electron back to PQ on the stromal side of the membrane, rendering a semiquinone in the  $Q_i$  pocket of the cytochrome ready as acceptor of another electron from PSII, and reduced cytochrome  $f$  feeds an electron to a water-soluble electron carrier, i.e. either plastocyanin or cytochrome  $c_{553}$ , for subsequent transfer to the reaction centre of PSI or to cytochrome  $c$  oxidase, respectively [90-94].

Electron transfer through the cytochrome  $b_6f$  complex proceeds according to the Q-cycle mechanism [90]. As a result, maximally 2 protons from the stroma are released into the lumen, per electron transferred. This electrochemical proton gradient can be used for the synthesis of ATP by the ATP-synthase complex [95]. In PSI another trans-thylakoid

membrane charge separation process is energized by light. Electron transfer within the PSI complex involves iron-sulphur clusters and quinones, and leads to reduction of ferredoxin, of which the reduced form serves as the electron donor for NADPH by the FNR enzyme [96]. The ATP and NADPH generated this way are used for CO<sub>2</sub> fixation, in a mutual stoichiometry that is close to the stoichiometry at which these two energy-rich compounds are formed at the thylakoid membrane. Normally this ratio is ATP:NADPH = 3:2 [97].

Photosynthetic- and respiratory electron transport in cyanobacteria share a single PQ pool [87,98-100]. Respiratory electron transfer provides cells the ability to form ATP in the dark, but this ability is not limited to those conditions: Transfer of electrons into the PQ pool is the result of the joint activity of PSII, respiratory dehydrogenases (in particular those specific for NAD(P)H and succinate), and cyclic electron transport around PSI [101-104], whereas oxidation of PQH<sub>2</sub> is catalysed by the plastoquinol oxidase, the cytochrome *b<sub>6</sub>f* complex, and by the respiratory cytochrome-c-oxidase [105-107], and possibly PTOX [108]. Multiple of these partial reactions can proceed simultaneously, including respiratory electron transfer during illumination [93], which includes oxygen uptake through a Mehler-like reaction [8,109].

Because of its central location in between the two photosystems, the redox state of the PQ pool has been identified as an important parameter that can signal photosynthetic imbalances [110-113]. Yet, an accurate estimation of the *in vivo* redox state of this pool has not been reported in cyanobacteria so far. Instead, the redox state of the PQ-pool is widely assumed to be reflected in, or related to, the intensity of the chlorophyll *a* fluorescence emissions [114-117]. Imbalance in electron transport through the two photosystems may lead to loss of excitation energy and hence to loss of chlorophyll *a* fluorescence emission [118]. Patterns of chlorophyll *a* fluorescence (pulse-amplitude modulated (PAM) fluorimetry [119]) have therefore widely been adopted for analysis of (un)balanced photosynthetic electron transfer, and by inference, for indirect recording of the redox state of the PQ-pool. However, the multitude of electron transfer pathways in the thylakoid membranes of cyanobacteria (see above) make it much more complex to explain PAM signals in these organisms than in chloroplasts [120]. Additional regulatory mechanisms of non-photochemical quenching, via the xanthophyll cycle in chloroplasts

[121] and the orange carotenoid protein [122] in cyanobacteria, and energy redistribution via state transitions [10,110], complicate such comparisons even further.

Several years ago, an HPLC-based technique was developed for the detection of the redox state of PQ(H<sub>2</sub>) in isolated thylakoids [123], but these results have neither been related to physiological conditions nor to the results of chlorophyll *a* fluorescence measurements. In this report we describe an adaptation of this method with elements of a method for estimation of the redox state of the ubiquinone pool in *Escherichia coli* [124]. This modified method allows for reliable measurements of the redox state of the PQ pool of *Synechocystis* sp. PCC 6803 under physiologically relevant conditions. The method uses rapid cell lysis in organic solvent to arrest all physiological processes, followed by extraction and identification of plastoquinol by HPLC separation with fluorescence detection. Next, we have manipulated the redox state of the PQ pool with various redox-active agents, with inhibitors of photosynthetic electron flow, and by illumination with light specific for either PSII or PSI. The measured redox state of the PQ pool was then related to the chlorophyll *a* fluorescence signal and 77K fluorescence emission spectra of cell samples taken in parallel and to oxygen exchange rates measured separately. These experiments reveal that - despite highly fluctuating conditions of photosynthetic and respiratory electron flow - a remarkably stable redox state of the PQ-pool is maintained. This homeostatically regulated redox state correlates poorly in many of the conditions tested with the more dynamical signal of chlorophyll *a* fluorescence emission, as measured with PAM fluorimetry. The latter signal only reflects the redox state of Q<sub>A</sub> and not of the PQ-pool.

## Results

### Method development for PQ- pool extraction and quantitative estimation

Established protocols for quantitative estimation of the amount of quinone and quinol present in extracts of rapidly-quenched intact cells, proved not directly applicable to cyanobacteria. In principle both plastoquinone and plastoquinol can be detected with HPLC through absorbance (255 nm) and fluorescence measurements (290 excitation, 330 emission), respectively. However, for technical reasons the maximal volume in rapid sampling had to be restricted to 2 ml. The amount of PQ that can be maximally extracted

from such a sample (approximately 1 nmol) gives a too low absorbance signal in our detection system for meaningful quantitation. Therefore we switched to the more sensitive detection of fluorescence emission from PQH<sub>2</sub> for the analysis of the extracts. Separation of PQH<sub>2</sub> from the other components in the extracts was done by HPLC; the peak eluting at 8.5 min (Fig. 2.1) was identified as PQH<sub>2</sub>, via comparison with a pure standard. For estimation of the *in vivo* PQ to PQH<sub>2</sub> ratio, quadruplicate samples were quenched immediately during the experiment, and at the end of each experiment an additional quadruplicate sample was taken and reduced with NaBH<sub>4</sub> before rapid extraction. For complete reduction of the PQ pool we observed that an amount of 2.5 mg NaBH<sub>4</sub> per µg of chl *a* is optimal (Fig. S2.1). The total size of the PQ pool does not change significantly over the course of a typical experiment with duration of 1 hour maximally (data not shown). The *in vivo* PQH<sub>2</sub> content was determined in the immediately quenched sample and the total PQ pool size *in vivo* was determined in the fully reduced sample. The *in vivo* redox state of the PQ pool is then expressed as  $[PQH_2] / ([PQ] + [PQH_2]) * 100 \%$ .

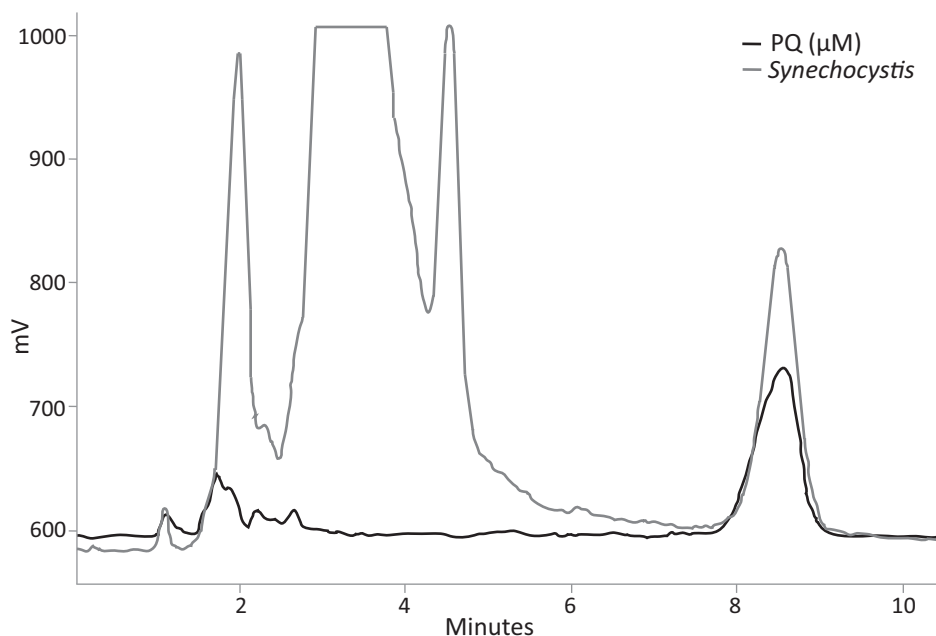


Figure 2.1. HPLC trace of a fully reduced 5 µM plastoquinol standard (black), and a fully reduced plastoquinol-containing extract from *Synechocystis* (grey). Samples were reduced with sodium borohydride (NaBH<sub>4</sub>). The peak in the extract eluting at 8.5 minutes co-elutes with the PQH<sub>2</sub> standard. Fluorescence excitation/emission was at 290/330 nm. The cut-off at 1000 mV is the upper detection limit of the system.

The relatively low midpoint potential of the plastoquinone/plastoquinol couple (+80 mV) made it necessary to protect PQH<sub>2</sub> against auto-oxidation. We found that the rate of oxidation of plastoquinol in methanol is so fast that methanol alone is unsuitable for plastoquinol extraction (Table 2.1). In contrast, petroleum ether (PE) proved to prevent oxidation of plastoquinol, and when PE was used as a 1:1 (v/v) mixture with methanol PQH<sub>2</sub> auto-oxidation in a 5 minute period was negligible. Therefore, this latter mixture was selected as appropriate solvent mixture for rapid extraction of PQH<sub>2</sub>. The extraction efficiency was tested at a chl *a* concentration of 3 mg L<sup>-1</sup> by repeating the PQ extraction steps four times and determining the PQ compound of each fraction. Under these conditions we found that the first and second fractions contained approximately 80 and 20 % of all PQ extracted, respectively, while the third and fourth fraction contain around 1.5 % and <0.5 %, respectively, (data not shown), from this we concluded that two extraction steps are sufficient. After extraction, the combined PE phases (see Materials and Methods) were immediately dried in a flow of N<sub>2</sub> and stored at -20 °C in 100 µl hexanol in an HPLC vial until processing. We observed that both for storage at low temperature and for subsequent analysis by HPLC, hexanol as a solvent showed the lowest auto-oxidation rates (Table 2.1). Shorter chain alcohols (ethanol, propanol, n-butanol) show higher rates and longer chains (octanol and decanol) do not significantly lower it. Alkanes and petroleum ether generate peaks in the HPLC chromatograms that distort the PQ peak (data not shown). Though hexanol was the most suitable solvent, it was not completely preventing auto-oxidation at room temperature (RT). For technical reasons HPLC had to be performed at RT and at this temperature PQH<sub>2</sub> in hexanol has an auto-oxidation rate of ~5 % per hour during the first three hours (Fig. S2.2). Therefore, we limited each HPLC run to a maximal run time of 2.5 hours. The data obtained is then corrected for the time the sample spent at RT in the auto-sampler, prior to HPLC analysis.

<b>solvent</b>	<b>half life</b>	<b>temp. (°C)</b>
<b>Methanol</b>	0.04 hours	4
<b>1:1 MeOH:PE</b>	∞	4
<b>Ethanol</b>	2.89 hours	21
<b>Hexanol</b>	9 hours	21
<b>Hexanol</b>	1565 hours	-20
<b>Hexanol</b>	376 hours	-80
<b>Dry</b>	84 hours	-20
<b>Dry</b>	232 hours	-80

Table 2.1. Half-life of PQH<sub>2</sub> (due to auto-oxidation) in different solvents at various temperatures. Oxidation was measured over a time course of 5 minutes at 4 °C, 8 hours at 21 °C and 24 hours at -20 and -80 °C. MeOH, methanol; PE, petroleum ether (40-60 °C). Data are from a typical experiment

### The redox state of the PQ pool in growing cells

To determine the effect of redox manipulations through changing physiological conditions on the *in vivo* redox state of the PQ pool, we tested both actively growing- and stationary-phase cells. We found that non-light-limited, fast growing *Synechocystis* cells have an oxidized PQ pool, while stationary-phase cells have a rather reduced PQ pool (Fig. 2.2). In between, during lower growth rates caused by light limitation, we consider a growth phase with an intermediate redox state of the PQ pool around OD<sub>730</sub> = 0.8. To be able to monitor both reduction and oxidation of the redox state of the PQ pool, this latter growth phase was selected for further experiments.

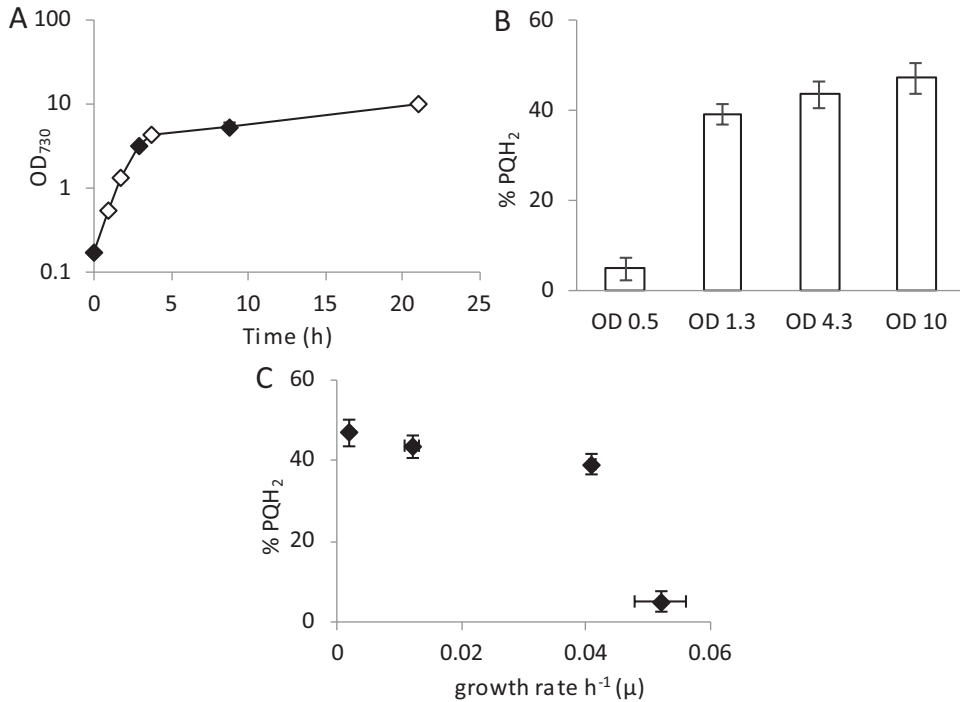


Figure 2.2. Growth curve of *Synechocystis* in batch culture in BG-11 medium with 25 mM NaHCO<sub>3</sub> (A) and the corresponding PQ redox states plotted against OD<sub>730</sub> (B) and growth rate per hour ( $\mu$ , C) at the four time points indicated with open diamonds in the growth curve. Error bars are standard deviation of biological duplicates.

### Redox-active reagents and inhibitors of photosynthetic electron flow

The quinone analogue DCBQ, in combination with 1 mM Fe<sup>3+</sup>, can take all electrons from PQH<sub>2</sub> and completely oxidize the pool to PQ; conversely NaBH<sub>4</sub> is a strong reducing agent that can convert all PQ into PQH<sub>2</sub>. Use of both chemicals permits one to mark the fully oxidized and the fully reduced state of the PQ pool, respectively. Setting of those conditions was confirmed through the plastoquinone extraction procedure (Fig. 2.3A). Figure 2.3B shows that addition of NaBH<sub>4</sub> raises chlorophyll *a* fluorescence to the F<sub>M</sub> level, while DCBQ does not affect the chlorophyll *a* fluorescence signal. Since the steady state fluorescence signal is close to F<sub>0</sub> in cells incubated in high carbon and moderate red light intensities (655 nm, 60  $\mu\text{mol photons m}^{-2} \text{s}^{-1}$ ), the DCBQ experiment was repeated with cells incubated in low carbon conditions and 100  $\mu\text{mol photons m}^{-2} \text{s}^{-1}$  red light (Fig. 2.3C). This figure shows that under these latter conditions DCBQ does lower the chlorophyll *a* fluorescence signal

but it does not approach  $F_0$ , as one would expect with a fully oxidized PQ pool, provided the fluorescence signal reflects the redox state of the PQ pool.

The photosynthetic electron transfer inhibitor DCMU has clear effects on the PAM signal (Fig. 2.3B). DCMU blocks the  $Q_A$  to  $Q_B$  electron transfer in PSII, which – in the light – causes complete reduction of  $Q_A$  and yields the maximal fluorescence signal. DCMU prevents electrons from PSII from flowing into the PQ-pool and thus would leave the PQ-pool fully oxidized, provided efflux of electrons, e.g. via PSI and/or the respiratory oxidases, continues. Although oxidation of the PQ-pool was observed in the presence of DCMU, some  $PQH_2$  still remained (Fig. 2.3A). DBMIB prevents outflow of electrons from the PQ-pool by blocking the  $Q_o$  site of the cytochrome *b<sub>6</sub>f* complex. With an active PSII this should cause strong reduction of the PQ-pool, which in turn would be expected to cause an increase in the chlorophyll *a* fluorescence signal. Addition of DBMIB does cause a strong rise in chlorophyll *a* fluorescence, followed by a slow drop and a stabilization of the signal at a level that is about twice as high as without addition (Fig. 2.3B). Interestingly, addition of DBMIB does not reduce the PQ-pool, if anything a small oxidation can be observed (Fig. 2.3A). This experiment was repeated under very low oxygen conditions ( $N_2$  sparging in the presence of glucose and glucose oxidase) and in the presence of 5 mM d-iso-ascorbic acid to fully reduce DBMIB beforehand; these latter experiments yielded similar results (data not shown).

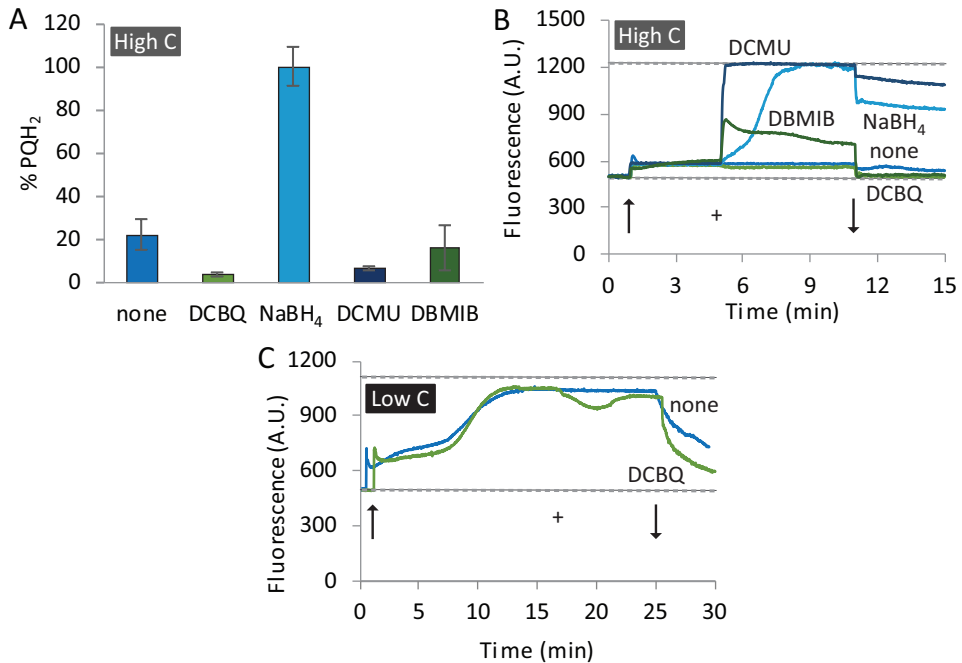


Figure 2.3. PQ redox state (A) and chlorophyll *a* fluorescence recordings (B, C) demonstrating the response of *Synechocystis* cells to addition of a range of different redox-active substances. PQ samples were taken 5 min after addition of each chemical; arrows indicate light on ( $\uparrow$ ) and light off ( $\downarrow$ ), the + sign indicates addition of the chemical. A and B: Experiments conducted in BG-11 with 50 mM NaHCO<sub>3</sub> and 60  $\mu\text{mol photons m}^{-2} \text{s}^{-1}$  655 nm light (referred as high-carbon conditions); C: Experiments conducted in BG-11 with 0.5 mM NaHCO<sub>3</sub> and 100  $\mu\text{mol photons m}^{-2} \text{s}^{-1}$  655 nm light (low-carbon conditions). Final concentrations: 10  $\mu\text{M}$  DCBQ + 1 mM K<sub>3</sub>Fe(CN)<sub>6</sub>; 2 mg ml<sup>-1</sup> NaBH<sub>4</sub>; 20  $\mu\text{M}$  DCMU; 0.5  $\mu\text{M}$  DBMIB. PQ redox state data (A) is an average of three independent experiments, error bars are standard deviation. Chlorophyll *a* fluorescence data (B,C) are from typical experiments.

### PQ redox state in PBS light only, and in PBS plus PSI light

In order to achieve different redox states in the PQ pool under physiological conditions we used different mixtures actinic light, absorbed by the phycobilisomes (PBS, 625 nm) and PSI (730 nm), respectively. Accordingly, an experiment was set up in which cultures with low- or high-carbon availability were illuminated with 100  $\mu\text{mol photons m}^{-2} \text{s}^{-1}$  625 nm light. After 25 minutes 25  $\mu\text{mol photons m}^{-2} \text{s}^{-1}$  730 nm light was added to the 625 nm illumination. Samples for analysis of the PQ redox state and for 77K fluorescence measurements were taken after 30 minutes in the dark and 10 minutes after the start of each of the illumination conditions. Figure 2.4A shows that the redox state of the PQ pool is somewhat more reduced in high-carbon- than in low-carbon conditions after 10 min 625 nm light, whereas in the dark the redox pool of the low-carbon sample is more reduced. This should be

compared with the massive difference in chlorophyll *a* fluorescence signals in 625 nm light (Fig. 2.4B). The small drop in chlorophyll *a* fluorescence and the increase in noise after addition of 730 nm light is an artifact caused by scattering of the 730 nm actinic light into the PAM detector and therefore no information could be extracted from the PAM signal in the presence of 730 nm illumination. The effect of 730 nm light on the redox state of the PQ-pool, however, can be interpreted: It is more reduced under 625 nm illumination than in darkness and becomes even more reduced when 730 nm light is added (Fig. 2.4B). The latter observation is counter-intuitive since one would expect that PSI-specific light will oxidize the PQ-pool.

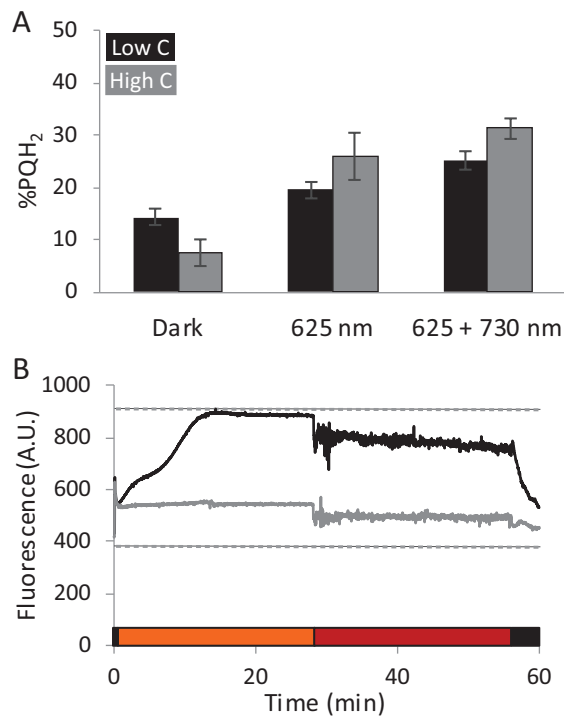


Figure 2.4. Redox state of the PQ-pool and chlorophyll *a* fluorescence emission of *Synechocystis* cells under various illumination conditions. Black: BG-11 medium with 0.5 mM NaHCO<sub>3</sub>; grey: BG-11 with 50 mM NaHCO<sub>3</sub>. A, PQ redox states; Samples were taken after 30 minutes in the dark, after 10 minutes in 100  $\mu\text{mol photons m}^{-2} \text{s}^{-1}$  625 nm light and 10 minutes after addition of 25  $\mu\text{mol photons m}^{-2} \text{s}^{-1}$  730 nm light. Data shown is the average of biological duplicates with standard deviation. B, chlorophyll *a* fluorescence recordings; orange bar, 100  $\mu\text{mol photons m}^{-2} \text{s}^{-1}$  625 nm light; red bar, 100  $\mu\text{mol photons m}^{-2} \text{s}^{-1}$  625 nm light with 25  $\mu\text{mol photons m}^{-2} \text{s}^{-1}$  730 nm light; black bar, dark; dashed lines,  $F_0$  and  $F_M$ .

At 77K the photosynthetic pigments are locked in place but they can still transfer their excitation energy to the photosystem they are bound to. By illuminating cell samples at 77K with light specific for PBS excitation and recording the fluorescence spectra we can get some insight to the level of coupling of the PBS to the photosystems. Fluorescence at 655 nm is emitted by phycocyanin (PC), fluorescence at 685 nm indicates coupling of the PBS to PSII and fluorescence at 720 nm coupling to PSI. Figure 2.5 shows that addition of 730 nm light triggers coupling of the PBS particularly to PSII in low-carbon medium (Fig. 2.5A), while with high carbon availability it triggers the release of PBS from, mainly, PSI (Fig. 2.5B).

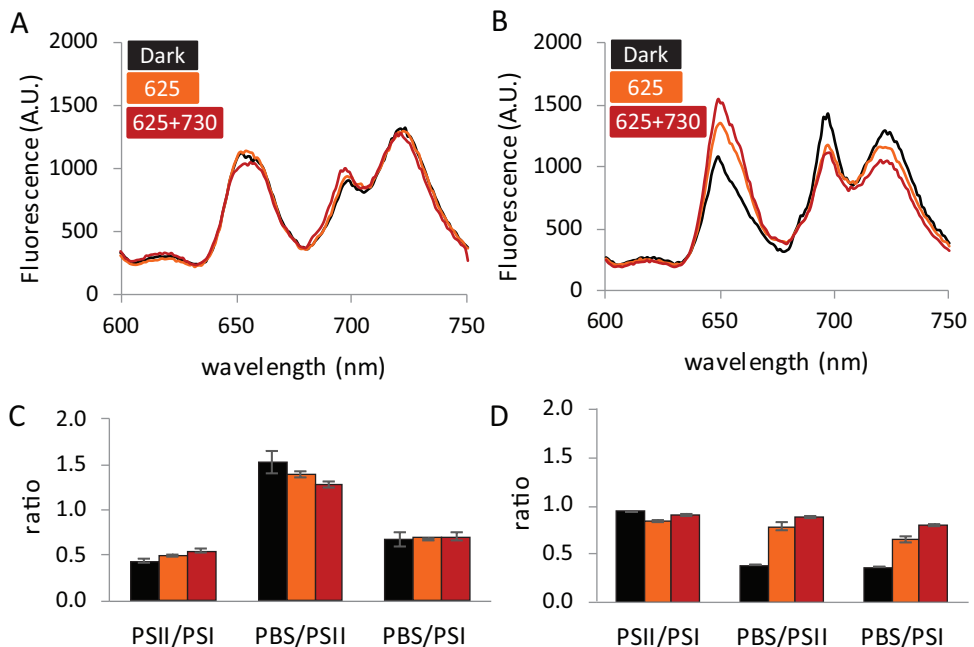


Figure 2.5. 77K fluorescence emission spectra, recorded with 590 nm excitation, of *Synechocystis* cells sampled under different conditions of carbon availability and illumination (A and B) and ratios of peak areas derived through skewed Gaussian de-convolution of these spectra (C and D). A and C: BG-11 with 0.5 mM NaHCO<sub>3</sub>; B and D: BG-11 with 50 mM NaHCO<sub>3</sub>. Black: Samples taken after 30 minutes in the dark; orange: samples taken after 10 minutes in 100  $\mu\text{mol photons m}^{-2} \text{s}^{-1}$  of 625 nm light; red: samples taken 10 minutes after addition of 25  $\mu\text{mol photons m}^{-2} \text{s}^{-1}$  of 730 nm light to a background of 100  $\mu\text{mol photons m}^{-2} \text{s}^{-1}$  of 625 nm light. The data shown in all panels is the average of biological duplicates; error bars in panel C and D are standard deviations. The peaks at 655, 685 and 720 nm are due to emission from phycocyanin (PC), PSII and PSI, respectively.

### **Oxygen evolution from PSII and selective activation of PSI with 730 nm light**

To further assess the effect of PBS- and PSI-specific illumination on the function of PSII we measured oxygen evolution rates. Use of oxygen evolution as a proxy for PSII performance in whole cells requires insight into oxygen uptake processes, to discriminate overall oxygen exchange from net oxygen production at PSII. The membrane inlet mass spectroscopy (MIMS) technique permits this. By adding a small amount of  $^{18}\text{O}_2$  gas to the culture we were able to detect oxygen uptake in the light, more details of this approach are presented in the Materials and Methods section. With an increasing 625 nm photon flux, addition of  $25 \mu\text{mol photons m}^{-2} \text{s}^{-1}$  730 nm light induces a large increase in the rate of oxygen evolution in cells with low-carbon availability (Fig. 2.6), allowing the cells to evolve oxygen at a rate that is comparable to cells in conditions of carbon excess. The  $P_{\text{max}}$  and  $\alpha$  values for this data were determined using sigmaplot (Table 2.2). Also, oxygen uptake in the light appears proportional to the amount of 625 nm light provided and exceeds respiration in the dark in all but the conditions with the lowest light intensities.

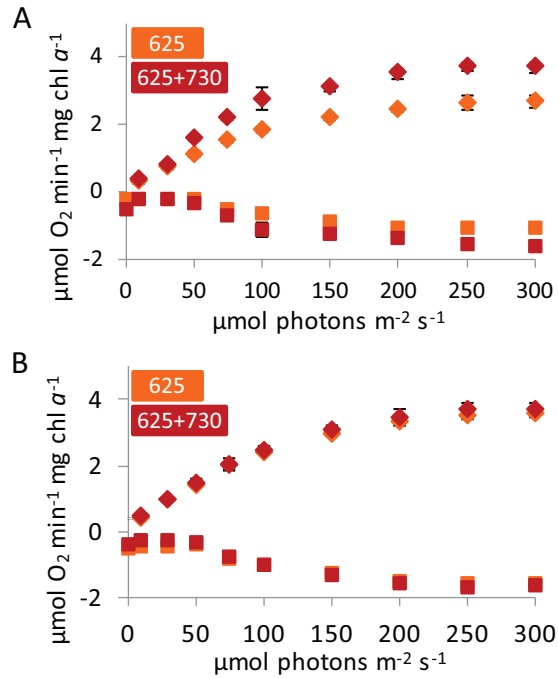


Figure 2.6. Oxygen evolution rates of *Synechocystis* cultures in increasing intensities of 625 nm light, recorded with MIMS.  $^{18}\text{O}_2$  was added at the start of the experiment to monitor oxygen consumption in the light. Depicted are: net photosynthesis (which is the sum of the measured  $\text{O}_2$  production and the consumption, (diamonds) and respiration (squares). A: BG-11 with 0.5 mM  $\text{NaHCO}_3$ ; B: BG-11 with 50 mM  $\text{NaHCO}_3$ . Orange: 625 nm light only; red: 625 nm light + 25  $\mu\text{mol photons m}^{-2} \text{s}^{-1}$  730 nm light. Data shown is the average of biological duplicates with standard deviation.

	$\alpha$	$\pm$	$P_{\max}$	$\pm$	$P_{\text{value}}$
<b>LC orange</b>	0.0228	0.0008	2.66	0.049	<0.0001
<b>LC far-red</b>	0.0324	0.0012	3.75	0.078	<0.0001
<b>HC orange</b>	0.0300	0.0009	3.60	0.060	<0.0001
<b>HC far-red</b>	0.0308	0.0010	3.75	0.067	<0.0001

Table 2.2.  $\alpha$  and  $P_{\max}$  values of net photosynthesis rates as depicted in figure 2.6, calculated with sigmaplot. LC, BG-11 with 0.5 mM  $\text{NaHCO}_3$ ; HC, BG-11 with 50 mM  $\text{NaHCO}_3$ ; orange, 625 nm light; far-red, 625 nm light with addition of 25  $\mu\text{mol photons m}^{-2} \text{s}^{-1}$  730 nm light.

## Discussion

In this study we have developed an extraction method with which we can reproducibly assay the *in vivo* PQ redox state of *Synechocystis* sp. PCC 6803. Because the extinction coefficient of plastoquinone is too small to detect this quinone in cell extracts by spectrophotometry, we measured its concentration indirectly by making use of the detection of fluorescence emission by plastoquinol (PQH<sub>2</sub>). To determine the PQ redox state in a cell culture, two sets of samples were taken and subsequently differently processed in quadruplo: One sample was the PQ/PQH<sub>2</sub> extracted as is, and the other was first completely reduced with NaBH<sub>4</sub> before extraction of PQH<sub>2</sub>. The difference in PQH<sub>2</sub> content in the two types of sample preparations is equal to the *in vivo* PQ redox state. The PQ redox state of the cells is defined as the ratio of the *in vivo* amount of PQH<sub>2</sub> over the total amount of plastoquinone/quinol, expressed as a percentage. It should be noted that because of this approach the method becomes relatively inaccurate when the PQ pool becomes very reduced (e.g. > 90 %). We observed, however, that the actual physiological reduction level of the PQ-pool never exceeded 50 % in our experiments. Hence, a substantial part of the PQ pool is always present as plastoquinone. Also, very small changes in the redox state of the PQ-pool cannot be monitored with our technique. In the permissible domain between 10 and 90 % the standard deviation ranges from 5 to about 10 %, and technical restraints (see Materials and Methods for more details) limit the number of parallel samples that can be analyzed for a given condition. Our data show that we can accurately detect transitions in the redox state of the PQ-pool from more reduced to more oxidized and *vice versa* in response to changes in the physiology of the *Synechocystis* cells. With the data we acquired we can also estimate the size of the PQ pool and how this size changes with growth phase. We found that each cell contains around 1.2 fg of plastoquinone and 27 fg chlorophyll *a* and that these values are stable in the range of  $5 \cdot 10^7$  to  $3 \cdot 10^8$  cells ml<sup>-1</sup> (i.e. in concomitantly measured OD<sub>730</sub> values range from 0.5 to 3; see Table 2.3). This implies that the PQ content of the cells does not change significantly between the linear light-limited growth phase and the phase of growth in which carbon limitation presumably starts to contribute. Only in stationary phase the PQ and chl *a* content per cell goes down (Table 2.3).

cell #	fg chl <i>a</i> cell <sup>-1</sup>	fg PQ cell <sup>-1</sup>	n
5·10 <sup>7</sup> - 3·10 <sup>8</sup>	27 ± 2.7	1.2 ± 0.33	17
4·10 <sup>8</sup> - 5·10 <sup>8</sup>	24 ± 0.1	0.8 ± 0.08	3
1·10 <sup>9</sup>	16	2	1

Table 2.3. Approximate amounts, in femtogram (fg), of chlorophyll *a* (chl *a*) and plastoquinone (PQ) per cell at different cell densities. N depicts the number of replicates the estimate was based on.

A basic assumption in this study has been that *Synechocystis* cells contain a single, homogenous, redox-equilibrated PQ pool. Nevertheless, several studies have shown that the distribution of protein components over the thylakoid membrane is non-homogenous [125,126] and between thylakoid and cytoplasmic membrane there are definitely differences in their abundance. This may cause differences in the activity of respiratory- and photosynthetic electron flow in these two types of membrane (but see: [100]). However, there is currently no evidence for the existence of local proton gradients. A further complication is that literature reports the existence in chloroplasts and cyanobacteria of an active and inactive plastoquinone pool, such that the inactive pool is located in small lipidic compartments called plastoglobuli. The inactive pool may comprise up to two-third of the total amount of plastoquinone in chloroplasts [123,127] and genes encoding plastoglobulin-related proteins have also been identified in *Synechocystis* [128].

Many studies in photosynthesis have used eukaryotic organisms (be it plants or (green) algae), in which oxidative phosphorylation (including respiratory electron transfer) and photosynthesis are separated into separate cellular organelles. In cyanobacteria, however, photosynthesis and respiration are intertwined and share PQ as a mobile electron carrier [87,99,100,129]. From this it follows that both photosynthetic- and respiratory electron flow determine the PQ redox state in cyanobacteria. This difference between cyanobacteria and chloroplasts may be the underlying reason for the observed strong homeostatic control of the redox state of the PQ pool of *Synechocystis* under a wide range of physiological incubation conditions that include anaerobiosis and exposure to high light intensities (see Results section and data not shown). The same broad spectrum of electron entry- and exit pathways that is present in cyanobacteria (see Introduction) is not available in chloroplasts of green algae and plants, although both some PQ reduction and PQ oxidation systems, called chlororespiration have been demonstrated in plant and microalgal chloroplasts [108,117,130-135]. Nevertheless, the experimental procedure of PQ pool

extraction that we present here can be applied in green algae as well, because the different types of quinones in mitochondria and chloroplasts permits their separate analysis with HPLC.

Our interest in the *in vivo* redox state of the PQ pool in cyanobacteria emerged from the relationship between the thylakoid redox state and several of the regulatory mechanisms that plants, micro-algae and cyanobacteria use to cope with dynamic changes in their environmental conditions, in particular light intensity. Quite some regulatory mechanisms and underlying signal transducing pathways have been attributed to the redox state of the PQ pool already [91,111,126,136-138]. With a strong homeostatic regulation and a highly stabilized PQ pool redox state, the proposed redox control of these regulatory processes may not be as straightforward to interpret as previously anticipated. Evidence acquired in this work includes the fact that the PSII inhibitor DCMU causes a maximal increase of chlorophyll *a* fluorescence by blocking  $Q_A$  to  $Q_B$  electron transfer, but this leads to only a partial oxidation of the PQ pool. This illustrates the active role of respiratory dehydrogenases, and cyclic electron flow around PSI [101,103,104] in the supply of electrons to the PQ pool. DBMIB prevents access of  $PQH_2$  to the  $Q_o$  pocket of the cytochrome *b<sub>6</sub>f* complex [139]. With PSII active, this should lead to an increase in the degree of reduction of the PQ-pool. However, this study shows that addition of DBMIB does not lead to reduction of the PQ pool (Fig. 2.3A). The binding of DBMIB shows only moderate affinity [90,140,141] and competition for the plastoquinol binding site depends on the redox state of DBMIB which can be modulated by the cells [90]. As the respiratory oxidases are insensitive to DBMIB, this allows electrons to exit the PQ pool even in the presence of this inhibitor [142]. It has been reported that DBMIB can cause oxidation of the PQ pool and that it can stimulate  $O_2$  uptake [140]. Also, oxidized DBMIB could function as an electron acceptor or a quencher of fluorescence [107]. So the experiment was repeated with DBMIB in the presence of 5 mM d-iso-ascorbate to fully reduce DBMIB prior to the experiment and in cultures that were continuously sparged with nitrogen and to which glucose and glucose oxidase was added. Even under these conditions DBMIB addition did not cause reduction of the PQ pool (data not shown).

Previous studies of a functional relation between the redox state of the PQ-pool and regulatory processes in the cells relied often on the use of inhibitors of photosynthetic

electron transport, such as DCMU and DBMIB. As demonstrated in this work, these agents do not exactly have the predicted effect on the redox state of the PQ pool in *Synechocystis*, which supports the notion that some of the regulatory processes are rather controlled via sensing of other components like the occupancy in the Q<sub>o</sub> or Q<sub>A</sub> site [112,143,144], and not by the redox state of the PQ-pool itself. However, the method used in this work cannot monitor the PQ redox state continuously; samples are taken manually and require immediate processing, making one sample per minute the maximal time resolution. So it is possible that addition of inhibitors or changes in the illumination conditions may result in rapid, but transient, changes in redox state to which the cell may respond.

Among the processes for which the signal transduction route urgently awaits clarification, and for which redox regulation has been implied, are e.g. the state transitions that regulate the distribution of photon energy over the two photosystems [10,145-148].

The impact of the redox active chemicals DCBQ ( $E_{m7} + 315$  mV) and NaBH<sub>4</sub> ( $E_m - 1.24$  V) that have an absolute effect on the redox state of the PQ pool is also reflected in the chlorophyll *a* fluorescence signal (Fig. 2.3B,C). NaBH<sub>4</sub> is a reducing agent, which should completely reduce the PQ pool, leaving no electron acceptors available for PSII. In this respect it is not surprising that addition of NaBH<sub>4</sub> results in a maximal chlorophyll *a* fluorescence signal, which is essentially similar to the level to which DCMU raises this fluorescence, which is consistent with the expectation that NaBH<sub>4</sub> will also fully reduce Q<sub>A</sub>. When the light is switched off in presence of NaBH<sub>4</sub> there is a steep drop in fluorescence, this goes against the idea that NaBH<sub>4</sub> will fully reduce Q<sub>A</sub>. However, the chl *a* fluorescence signal in cyanobacteria is in part distorted by fluorescence from unbound PBS [120]. This could, in part, explain the sudden drop in fluorescence. In contrast, addition of DCBQ (in the presence of Fe<sup>3+</sup>) takes all the electrons out of the PQ pool [149] but only slightly lowers the chlorophyll *a* fluorescence signal and only when this signal is high to start with. In low-carbon medium there is an imbalance between ATP supply and electron acceptor availability. Generally, lack of CO<sub>2</sub> is accompanied by an increase in Q<sub>A</sub> reduction level (and therefore a strong increase in the chlorophyll *a* fluorescence signal, see above) but also a higher resistance to photoinhibition [150]. Under conditions of high excitation pressure there is increased cyclic electron flow around PSII via cytochrome *b*<sub>559</sub> [151]. It has also been shown that in low-carbon conditions the flavodiiron proteins Flv2 and Flv4 help

protect PSII by accepting electrons from the reaction center [152,153]. Transfer of electrons to cytochrome  $b_{559}$  is much slower than transfer to the PQ pool, this could lead to accumulation of reduced  $Q_A$  which would explain the high fluorescence level. DCBQ is a general quinone analogue and it would certainly be possible for DCBQ to accept electrons from cytochrome  $b_{559}$  or even from  $Q_A$  or  $Q_B$  directly. This would alleviate the backpressure on PSII and explain the drop in chlorophyll  $a$  fluorescence in low-carbon conditions. Hence, while chlorophyll  $a$  fluorescence measurements report about the redox state of the plastoquinone in the  $Q_A$  site of PSII, the redox state of this component may differ from the redox state of the PQ pool.

The direct comparison between the redox state of the PQ pool with the intensity of the chlorophyll  $a$  fluorescence signal under a range of physiological conditions further demonstrates the poor correlation between these two parameters (e.g. Fig. 2.4). To further illustrate their lack of direct correlation, a typical discrepancy between the two is shown in 625 nm light (that selectively excites the PBS), in which the PQ pool is somewhat more reduced in high-carbon conditions than it is in low-carbon conditions, while the chlorophyll  $a$  fluorescence signal is much lower in high-carbon conditions (Fig. 2.4). This discrepancy is most likely caused by up-regulation of cyclic electron flow around PSII which lowers the electron transfer to the PQ pool and further supports our interpretation that the redox state of  $Q_A$  and of the PQ pool are not directly correlated to one another. In the redox midpoint potentials on the acceptor side of PSII a clear gradient is observed:  $Q_A/Q_A^- \approx -100$  mV [83,84];  $Q_B/Q_B^- \approx 0$  mV [85] and the  $PQH_2/PQ$  pool = + 80 mV [88]. Hence, it is understandable that if for some reason kinetics of electron transfer in the initial part of the Z-scheme are impaired, the correlation between the redox state of  $Q_A$ ,  $Q_B$  and the PQ pool is lost.

Further studies of the effect of additional PSI light on this correlation were hampered by limitations of our equipment to measure chlorophyll  $a$  fluorescence. With a chlorophyll  $a$  extract in 80 % acetone, with added milk powder to introduce light scatter, we confirmed that the initial drop that we observe in the PAM signal (Fig. 2.4B) after the addition of 730 nm light is an artefact in the form of an offset of the PAM measuring system (data not shown).

We expected the PQ pool to be more oxidized in the presence of PSI-specific illumination because this light should enable PSI to oxidize the PQ pool at a higher rate. However, this was not observed (Fig. 2.4A). The dynamically variable connection of the PBS antenna to either PSII, PSI, or to neither of these two, was considered as a possible cause. We therefore analyzed fluorescence excitation- and emission spectra recorded at 77K. These confirm that PSI-specific light triggers a state 1 transition (Fig. 2.5). Especially in low carbon conditions, the light to dark state transition in *Synechocystis* is small (Fig. 2.5), compared to the corresponding transition in other species such as *Synechococcus* [120]. Species in which state transitions, and therefore energy redistribution, are more pronounced may also display stronger variations in PQ pool redox state. Mullineaux and Allen [111] have proposed that state transitions in cyanobacteria are triggered by changes in the redox state of the PQ pool, or of a closely associated electron carrier, but later others have ascribed this trigger function to the plastoquinone in the  $Q_o$  site of the  $b_6f$  complex [144,154]. Here we see that cells which are in state 1 have a more reduced PQ pool – rather than a more oxidized one - than cells that are in state 2. I.e. regardless of whether redox related triggers sense the redox state of PQ, or the occupation of the  $Q_o$  and/or the  $Q_A$  site, this sensing mechanisms cannot respond to the steady state redox level of the PQ pool. Conditions such as low-carbon availability and high light intensities induce many protective mechanisms to limit the amount of electrons liberated from water, such as non-photochemical quenching of PSII [155], state transitions [111], cyclic electron flow around both photosystems [114,156] and energy quenching mechanisms such as those facilitated by the orange carotenoid protein (OCP, [122]) and the flavodiiron proteins 2 and 4 [152,153]. This means that despite the high excitation pressure in low-carbon conditions, the cells in high carbon conditions are at a greater risk of over-reduction of the PQ pool if PBS binding to PSII is increased. This may explain the difference in the mechanism underlying the state transitions: The state 1, observed in high-carbon conditions, is achieved mainly by uncoupling of PBS from PSI, while the state 1, observed in low-carbon conditions, is based on coupling of PBS to PSII (Fig. 2.5 C, D), for an overview see figure S2.3. Further studies with sodium fluoride (a phosphatase inhibitor [157]) or the use of mutants impaired in state transitions may help to disclose in greater detail this versatility in relative PBS binding to the two photosystems in *Synechocystis*.

Although the occurrence of a state 1 transition may not be convincing from the 77K data alone, the oxygen evolution experiments (Fig. 2.6) show the strong contribution from low intensity 730 nm light. While carbon limitation represses oxygen evolution from PSII, addition of low intensity 730 nm light completely abolishes this effect; lifting the oxygen evolution (rate) up to the same level as in carbon replete conditions. Addition of 730 nm light will accelerate PSI activity and may increase the rate of cyclic electron flow around PSI. Via increased ATP synthesis this will lower the NADPH:ATP ratio, and make extra ATP available for active  $\text{HCO}_3^-$  uptake [158]. The increased PSI activity and, possibly, higher availability of  $\text{CO}_2$  for carbon fixation will increase the turnover rate of PSII, in combination with the increased PBS coupling, induced by the state 1 transition, explain the benefit of additional PSI light to cultures in low-carbon conditions, and possibly under ATP-stress in general. Finally, the oxygen uptake rates of *Synechocystis* in the light are higher than the respiration rates in the dark. An often-made assumption holds that the rate of oxygen uptake in the light never will exceed the corresponding dark respiration (see e.g. [159]), although there have been previous reports that this assumption does not always hold [8,160,161]. To maintain a fairly oxidized PQ-pool redox state, it may be necessary for the cell to dissipate quite a lot of redox energy (i.e. transfer electrons to oxygen) to prevent over-reduction of the electron transfer system. By using respiratory enzymes for this the cell can still use the free energy of these electrons for the production of ATP. Moreover, Helman et al. [109] have shown that up to 40 % of the electrons extracted from water by PSII are directly transferred back to oxygen (to re-form water) via a flavoprotein-catalyzed Mehler-like reaction. Allahverdiyeva et al. [8] further stress the importance of this reaction in cyanobacteria. In this way, a customized combination of linear- and cyclic electron flow and respiration allows the cell to balance its ATP and NADPH supply, according to the needs dictated by its physiology and its environment.

The largest variation in the redox state of the PQ-pool observed in this study was in the different stages of growth (Fig. 2.2). With a non-limiting supply of light and nutrients, photosynthesis can run at its highest capacity (and indeed cellular growth is exponential) during the first one or two days. This very rapid electron flow through the Z-scheme apparently leads to a highly oxidized PQ pool. When light and/or nutrients start to become

limiting the flow through the system will slow down, and the homeostatic regulatory mechanisms kick in.

It appears that for cyanobacteria the ability to homeostatically regulate the redox state of its PQ pool is more important than preserving maximum amounts of free energy in the form of NADPH and ATP. Since cyanobacteria thrive in open water columns, in which mixing can suddenly expose them to high light intensities and/or nutrient limitation, this mode of regulation may very well be an important survival strategy.

## Materials and Methods

### Strains and culture conditions

*Synechocystis* sp. PCC 6803 was grown in a continuous culture photo-bioreactor [162] with a volume of 1.8 liter and a light-penetration of 5 cm at a temperature of 30 °C. Growth was in continuous red LED-light (650 nm, 60  $\mu\text{mol photons m}^{-2} \text{ s}^{-1}$  incident light) in BG-11 mineral medium [163] complemented with 15 mM  $\text{Na}_2\text{CO}_3$ . Mixing was established with a stream of sparged air, enriched with 2 %  $\text{CO}_2$  at a rate of 30 L  $\text{h}^{-1}$ . The dilution rate was set to 0.015  $\text{h}^{-1}$ , and a light-limited steady state with a final culture density of  $8 \cdot 10^7$  cells  $\text{ml}^{-1}$ , an  $\text{OD}_{730}$  of 0.8 and 2 mg chlorophyll (chl)  $a \text{ L}^{-1}$  was reached.

For experiments in which the PQ pool redox state was manipulated aliquots of the culture (between 50 and 300 ml) were taken and centrifuged (5 min, 1500g), washed once in BG-11 complemented with 0.5 or 50 mM  $\text{NaHCO}_3$  (referred to as low- and high-carbon medium, respectively) and resuspended in the same medium to a chl  $a$  concentration of 2 mg  $\text{L}^{-1}$ .

To study the PQ pool redox state during growth, batch cultures were inoculated at an  $\text{OD}_{730}$  of 0.1 in BG-11 medium complemented with 25 mM  $\text{NaHCO}_3$ . The cells were grown at 30 °C in a shaking incubator at 200 rpm under 30  $\mu\text{mol photons m}^{-2} \text{ s}^{-1}$  of plant-specific fluorescent light (Sylvania Gro-Lux).

### Sampling under varying light conditions

*Synechocystis* cultures in low- or high-carbon medium with a chl  $a$  concentration of 2 mg  $\text{L}^{-1}$  were placed in a 300 ml flat panel culture vessel with a light-path of 3 cm. The vessel was placed in between two LED light sources to ensure a constant light climate inside the vessel.

The monitoring optical fiber of the PAM was placed against the side of the vessel, perpendicular to the light sources. The vessel was equipped with a rapid sampler, used for PQ redox state determination, as well as a long needle connected to a 1 ml syringe for sampling for 77K fluorescence emission spectroscopy (further detail see below). At the start of the experiments the cultures were dark-adapted for 30 minutes, after which samples for 77K spectroscopy, PQ redox state analysis and optical density measurements were taken and the  $F_0$  and  $F_M$  of the PAM signal were determined with a saturating pulse generated by the LED lamps (for further detail: see below). The cultures were then exposed to 625 nm (phycobilisome) light, which preferentially excites PSII, at an intensity of  $100 \mu\text{mol photons m}^{-2} \text{ s}^{-1}$  and after 10 min samples for 77K spectroscopy and for PQ-pool extraction were taken. After 25 minutes in 625 nm light only,  $25 \mu\text{mol photons m}^{-2} \text{ s}^{-1}$  of 730 nm LED light for excitation of PSI was added to the 625 nm light and after another 10 minutes 77K- and PQ samples were collected again. The PAM signal was monitored continuously.

#### **Chemical agents used for modulation of the redox state of the PQ-pool**

The effect of addition of various chemicals has been tested in aliquots of cultures incubated in the light, and samples were taken 5 minutes after each addition. Final concentrations were;  $2 \text{ mg ml}^{-1}$  sodium borohydride ( $\text{NaBH}_4$ , Sigma),  $10 \mu\text{M}$  2,6-dichloro-p-benzoquinone (DCBQ, Kodak) with addition of 1 mM potassium ferricyanide ( $\text{K}_3\text{Fe}(\text{CN})_6$ ) to allow re-oxidation of DCBQ,  $20 \mu\text{M}$  3-(3,4-dichlorophenyl)-1,1-dimethylurea (DCMU, Sigma) and  $0.5 \mu\text{M}$  2,5-dibromo-3-methyl-6-isopropyl-p-benzoquinone (DBMIB, Sigma).

#### **Plastoquinol detection by HPLC**

By use of a rapid sampling device [164] two ml cell culture was rapidly sampled (within 0.5 s), directly into the extraction agent, which consists of a 12 ml ice-cold ( $4 \text{ }^\circ\text{C}$ ) 1:1 (v/v) mixture of methanol and petroleum ether (PE, bp range  $40\text{-}60 \text{ }^\circ\text{C}$ ). This ensured not only reproducible and quantitative sampling but most importantly freezing of the *in vivo* redox state of the cells. Then the sample was thoroughly mixed in capped glass tubes (vortex) for 1 minute. The mixture was then immediately centrifuged ( $900 \text{ g}$ , 1 min,  $4 \text{ }^\circ\text{C}$ ), and the upper petroleum ether phase was transferred to a  $\text{N}_2$  flushed glass tube. To the remaining lower phase 3 ml petroleum ether was added for a second extraction, and the mixing and centrifugation steps were repeated. The collected PE upper phases were combined and the

PE was evaporated to dryness under a flow of N<sub>2</sub> at room temperature. The dried extract was re-suspended in 100 µl hexanol and stored at -20 °C until analysis by HPLC, using a Pharmacia LKB gradient pump 2249 system. The instrument was equipped with a fluorescence detector (Agilent 1260 infinity FLD) and a reverse-phase Lichrosorb (Chrompack) 10 RP 18 column (4.6 mm i.d., 250 mm length). The column was equilibrated with pure methanol which was also used as the mobile phase. The flow rate was set at 2 ml min<sup>-1</sup>. Fluorescence excitation/emission was at 290/330 nm. Methanol (Sigma), hexanol (Sigma) and petroleum ether (Biosolve) were of analytical grade. The presence of plastoquinol was confirmed with a plastoquinone-9 standard kindly provided to us by Dr. Jersey Kruk. Plastoquinone was reduced with NaBH<sub>4</sub> prior to HPLC analysis.

### **PQ reduction**

In order to determine the redox state of the PQ pool, the total amount of PQ (i.e. sum of plastoquinol + plastoquinone in the sample) for each condition was determined by fully reducing 2 ml of the cell culture at the end of each experiment with 5 mg ml<sup>-1</sup> NaBH<sub>4</sub>, 1 minute before rapid extraction, and subsequent HPLC analysis. The redox state of the PQ pool was then determined from the difference between the area of the peaks obtained from physiologically reduced (A) cells and fully (i.e. NaBH<sub>4</sub>) reduced (A<sub>M</sub>) cells; (A/A<sub>M</sub>). In this approach we assume that - due to rapid disproportionation - any plastosemiquinone formed in the non-protein bound PQ pool will instantaneously be converted into a combination of PQ and PQH<sub>2</sub>. The redox state of the PQ pool is presented as % reduced (i.e. PQH<sub>2</sub>) of the total PQ pool.

### **Fluorescence measurements**

Measurements of PSII fluorescence were performed with a PAM-100/103 instrument (Walz, Germany). F<sub>0</sub> and F<sub>M</sub> were determined directly on the sample vessel after a dark incubation of 30 minutes using the light source of the photobioreactor switched on at maximum intensity (6000 µmol photons m<sup>-2</sup> s<sup>-1</sup>). Steady state fluorescence (i.e. F<sub>t</sub>) was recorded under a range of different illumination conditions.

### **77K fluorescence analysis**

For 77K fluorescence analysis samples were taken from different illumination conditions and diluted 4 times in ice-cold medium with glycerol (final concentration 30 % (v/v)) and

immediately frozen in liquid nitrogen. The samples were analyzed in an OLIS 500 spectrofluorimeter, equipped with a Dewar cell. PBS-specific excitation light was used at 590 nm, and fluorescence emission spectra were recorded between 600 and 750 nm, a wavelength domain in which the PBS (655 nm), PSII (685 nm), and PSI (720) show well-separated emission peaks. Skewed Gaussian de-convolution was performed on the different peaks in order to assay the degree of coupling of the PBS to PSII and PSI.

### **MIMS measurements**

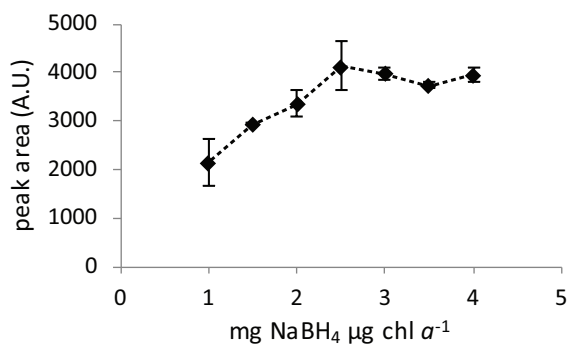
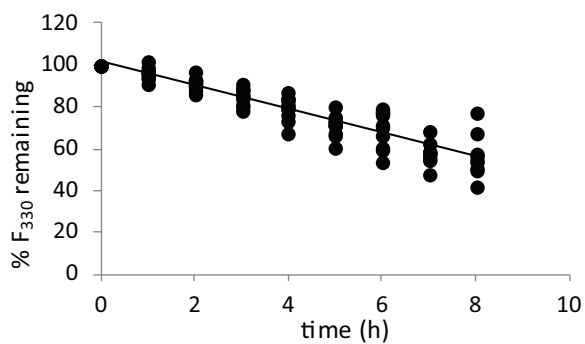
Membrane inlet mass spectrometry measurements were performed using a HPR-40 system (Hiden Analytical Ltd, Warrington, England) in a 10 ml air tight cuvette (a modified DW3 cuvette from Hansatech Instruments Ltd) containing a *Synechocystis* culture in low- or high-carbon medium, with a density of 2 mg ml<sup>-1</sup> chl *a*. The high-vacuum membrane inlet sensor of the mass spectrometry analyzer was placed in the liquid culture. A thin medical grade silicon tubing serving as membrane secured continuous passage of small amounts of gasses from the liquid phase into the sensor tube of the mass spectrometer. Prior to the experiment the sample was dark adapted for 30 minutes, and then briefly ( $\pm 10$  sec) sparged with N<sub>2</sub> to reduce the prevalent O<sub>2</sub> concentration to about 20 % of the value in air-equilibrated incubation buffer, with the aim to prevent O<sub>2</sub> saturation during the experiment. After sparging, the cuvette was closed and 1 ppm of <sup>18</sup>O<sub>2</sub> (95-98 % pure, Cambridge Isotope Laboratories Inc) was added in the head space which, while stirring, equilibrated with the liquid. An up-sloping mass spectrometer signal denoted the dissolving <sup>18</sup>O<sub>2</sub>, until a plateau was reached. When the desired concentration was reached (10-15 % of the total O<sub>2</sub>-concentration), the chamber was sealed after removing the <sup>18</sup>O<sub>2</sub> bubble. In order to minimize noise the signals were normalized to Argon as suggested by Kana et al. [165]. For more information on the calculation procedure see [166]. The cultures were subjected to increasing 625 nm light intensities, ranging from 10 to 300  $\mu\text{mol photons m}^{-2} \text{s}^{-1}$  in steps of 20  $\mu\text{mol photons m}^{-2} \text{s}^{-1}$  below 100  $\mu\text{mol photons m}^{-2} \text{s}^{-1}$  and steps of 50  $\mu\text{mol photons m}^{-2} \text{s}^{-1}$  above 100  $\mu\text{mol photons m}^{-2} \text{s}^{-1}$ , aimed to excite PSII via its attached phycobilisomes. This illumination was combined with (or without) addition of 25  $\mu\text{mol photons m}^{-2} \text{s}^{-1}$  of 730 nm light, which typically only excites PSI. The lowest light intensity at the start of the experiment was on for a period of 10 minutes, to secure light adaptation,

The redox state of the PQ pool of *Synechocystis* is under strict homeostatic control and all subsequent light intensities were kept on for 3 minutes. After the incubation in the light, dark respiration was monitored for 10 minutes.

## **Acknowledgements**

We would like to thank Jersey Kruk for providing us with a pure standard of plastoquinone-9 and Ivo van Stokkum for help in the analysis of the 77K fluorescence emission data.

## Supplemental Material

Figure S2.1. Reduction of PQ with different quantities of  $\text{NaBH}_4$ .Figure S2.2. Oxidation of  $\text{PQH}_2$  in hexanol over time.

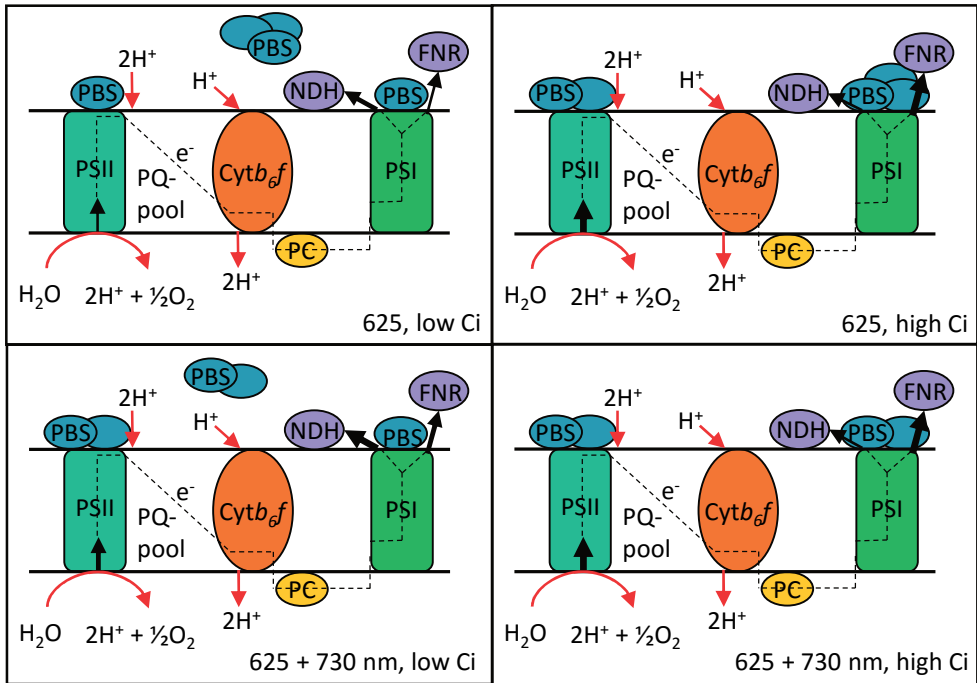


Figure S2.3. Cartoon of PBS binding under different light and carbon conditions. Dashed lines show the electron flow, black arrows show the direction and the strength of the electron flow. Proton translocation is shown with red arrows for 1 water molecule. PBS, phycobilisomes; PC, plastocyanin; FNR, ferredoxin:NADP<sup>+</sup> reductase, NDH, NADPH dehydrogenase or cyclic electron flow. Low Ci, low carbon conditions; high Ci, high carbon conditions.